HHS Public Access

Author manuscript

J Immunol. Author manuscript; available in PMC 2021 January 01.

Published in final edited form as:

J Immunol. 2020 January 01; 204(1): 49–57. doi:10.4049/jimmunol.1900440.

DOCK2 sets the threshold for entry into the virtual memory CD8+ T cell compartment by negatively regulating tonic TCR triggering

Vinay S Mahajan[*,1,2], **Ezana Demissie**[*,1], **Faisal Alsufyani**[1,3], **Sudha Kumari**[4], **Grace J Yuen**[1], **Vinayak Viswanadham**[1], **Andrew Huang**[1], **Johnson Q. Tran**[5], **James J. Moon**[5], **Darrell J Irvine**[1,4], **Shiv Pillai**[1]

[1]Ragon Institute of MGH, MIT and Harvard, Cambridge MA

[2]Brigham and Women's Hospital, Boston MA

[3]King Fahad Specialist Hospital, Dammam, Saudi Arabia

[4]The Koch Institute for Integrative Cancer Research at MIT, Cambridge MA

[5]Center for Immunology and Inflammatory Diseases, Massachusetts General Hospital

Abstract

The control of cytoskeletal dynamics by Dedicator of cytokinesis 2 (DOCK2), a hematopoietic cell-specific actin effector protein, has been implicated in TCR signaling and T cell migration. Biallelic mutations in *Dock2* have been identified in patients with a recessive form of combined immunodeficiency with defects in T, B and NK cell activation. Surprisingly, we show here that certain immune functions of $CD8^+$ T cells are enhanced in the absence of DOCK2. *Dock2*-deficient mice have a pronounced expansion of their memory T cell compartment. Bone marrow chimera and adoptive transfer studies indicate that these memory T cells develop in a cell-intrinsic manner following thymic egress. Transcriptional profiling, TCR repertoire analyses and cell surface marker expression indicate that *Dock2*-deficient naive $CD8^+$ T cells directly convert into virtual memory cells without clonal effector T cell expansion. This direct conversion to memory is associated with a selective increase in TCR sensitivity to self-peptide MHC *in vivo* and an enhanced response to weak agonist peptides *ex vivo*. In contrast, the response to strong agonist peptides remains unaltered in *Dock2*-deficient T cells. Collectively, these findings suggest that the regulation of the actin dynamics by DOCK2 enhances the threshold for entry into the virtual memory compartment by negatively regulating tonic TCR triggering in response to weak agonists.

INTRODUCTION

We have previously described a loss-of-function *Dock2* allele ($Dock2^{hsd}$) that had been inadvertently introduced into multiple mouse lines (1). Using this knockout allele of *Dock2* extensively in this study, we find that the responsiveness of *Dock2*-deficient $CD8^+$ T cells to weak agonists is unexpectedly enhanced. Thus, while DOCK2 may promote TCR responses to strong agonists, it appears to constrain the responsiveness to weak TCR agonists. *In vivo*, the loss of DOCK2 results in an enhanced conversion to virtual memory T cells. Virtual

[*]Equal contributors

memory T cells can provide antigen-independent innate-like bystander protection in the context of intracellular infection against some pathogens such as *Listeria monocytogenes* (2), and contribute to protective immunity in mice (3, 4). In this present study, we show that the memory phenotype T cells, previously shown to be expanded in the absence of DOCK2 (1), are polyclonal virtual memory cells and demonstrate that they are generated by direct conversion of naive T cells into memory as a result of cell-intrinsic hyperresponsiveness of *Dock2*$^{hsd/hsd}$ T cells to weak agonists. Mice with other engineered *Dock2* mutations also exhibit the same phenotype. These findings suggest that the absence of DOCK2 lowers the threshold of self-peptide triggering required to enter the virtual memory T cell compartment.

Aside from homeostatic cytokine signaling and tonic TCR triggering, very little is known about the regulators of the CD8$^+$ T cell virtual memory compartment. FYB1 (Fyn binding protein 1) has been proposed to function as a negative regulator of the size of the CD8$^+$ virtual memory compartment by limiting the response to IL-15 (5). This study shows that DOCK2 functions as a novel negative regulator of the CD8$^+$ virtual memory compartment. DOCK2 (Dedicator of cytokinesis 2) activates the actin effector Rho GTPase Rac by catalyzing the transition from the inactive GDP-bound state to the active GTP-bound state (6). DOCK2 localizes to the cell membrane via its DHR1 domain mediated interactions with PIP3 and polybasic amino acid cluster based interactions with phosphatidic acid, thus ensures spatially controlled activation of GTPase Rac at the plasma membrane (6-8). GTP bound RAC1 subsequently drives actin polymerization enabling cytoskeletal rearrangements required for lymphocyte chemotaxis (6, 9, 10), T cell interstitial motility (11), plasmacytoid dendritic cell cytokine secretion (12), and TCR activation (13, 14). This study suggests that DOCK2-dependent remodeling of actin cytoskeletal may limit the responsiveness of CD8 T cells to weak agonists such as self-peptides, thereby regulating the size of the virtual memory compartment.

MATERIALS AND METHODS

Mice

Dock2$^{hsd/hsd}$ mice were purchased from Harlan Laboratories and maintained as a separate colony in a specific pathogen free environment in accordance with institutional guidelines. C57BL/6J, OT-I and RAG1 knockout mice were purchased from Jackson Laboratory. Unless otherwise specified, all experiments were conducted using 8-12 week-old mice.

Bone marrow chimeras

Bone marrow was isolated from the indicated mice. Resuspended cells from the bone marrow were labeled using biotinylated anti-CD3 antibody and streptavidin microbeads (Miltenyi Biotec). Cells were then resuspended in PBS and 1×10^6 cells were transferred to each mouse.

Cell transfers

For lymphopenia induced proliferation experiments, mice were irradiated at a dose of 600 cGy. 6 hours later, a total of $1X10^6$ CFSE labeled naive T cells from *Dock2*$^{hsd/hsd}$ and WT

mice were co-injected into irradiated congenic hosts. One week later, transferred cells were recovered and assessed for CFSE dilution and CD44 upregulation.

For experiments in lymphoreplete mice, a total of 2×10^6 naive T cells from *Dock2*$^{hsd/hsd}$ and WT mice were co-injected into unmanipulated congenic hosts. Three weeks later, transferred cells were assessed for CD44 and CD122 upregulation.

RNA Sequencing and TCR repertoire analysis

RNA from 50,000 cells for each condition was isolated with QIAGEN RNA isolation kits according to the manufacturer instructions. RNA-Seq libraries were then prepared using the Smart-Seq2 protocol (43). Libraries were sequenced on an Illumina NextSeq 550. Paired end reads were aligned to the mm10 reference genome and expected transcript counts were estimated using the RSEM package. The transcriptomic data is available at the NCBI GEO database (https://www.ncbi.nlm.nih.gov/geo/query/acc.cgi?acc=GSE135594). Gene Set Variation Analysis (GSVA) as well as Gene Set Enrichment Analysis (GSEA) were used to determine if the naïve $CD8^+$ T cell gene expression program matched known immunological gene expression signatures (25, 26, 44). Differentially enriched gene sets were identified using the Limma package (45). From each mouse, 50,000 naïve or memory phenotype CD8 T cells were sorted and the extracted RNA was used to prepare TCR repertoire libraries using a commercially available iRepertoire kit for mouse TCRβ and sequenced on an Illumina MiSeq instrument. V, D and J segment assignment and clonotypes identification was performed using MiXCR (46). Repertoire sequencing metrics are included in Supplementary Table 3. VDJtools was used for post analysis determination of convergence, diversity and hierarchical clustering of samples based on TCR Vβ usage (27).

T cell stimulation

Ex vivo polyclonal stimulation was performed by incubating T cells in a cell stimulation cocktail from eBioscience (cat: 00-4975-03) for 4 hours. Cytokines were purchased from Peprotech and used at a concentration of 10 ng/ml for 18 hours. For OT-I TCR stimulation altered peptide ligands were synthesized by AnaSpec and used at the indicated concentrations to stimulate cells for 4 hours.

Listeria infection

Mice were intravenously infected with 2×10^4 CFUs of LM10403S. At the indicated times, livers were homogenized with 0.05% Triton-X in PBS followed by plating of serial dilutions on Brain Heart Infusion agar plates containing streptomycin.

Flow cytometry

The following antibodies were used for surface staining CD8 (53-6.7), CD44 (IM7), CD49d (R1-2), CD122 (TM-β1), IFN-g (XMG1.2), CD69 (H1.2F3), CD25 (, Ki67 (16A8), TCR, Vβ5 (MR9-4), Vα2 (B20.1), CD45.1 (A20), CD45.2 (104), CD90.1 (OX-7), CD90.2 (30-H12). Cells were permeabilized for intracellular staining using the Foxp3 permeabilization kit (eBioscience cat:00-5523-00).

Microscopy and image analysis

OT-I T cells tagged with fluorescently labeled anti-CD8 nanobodies were co-cultured for 4 hours in the presence of antigenic peptide-loaded syngeneic wild-type bone-marrow derived dendritic cells generated from B6 bone marrow (47, 48). The cells were fixed, stained and imaged using confocal microscopy as previously described (32). Image processing was carried out using ImageJ and Metamorph software. To assess F-actin intensity, the region of interest was defined as corresponding to the zone of actin polymerization along the contact interface between T cell and dendritic cell, and the F-actin intensity was quantified using MetaMorph Software. All images presented here are raw images, displayed at identical contrast settings.

RESULTS

Absence of DOCK2 results in the expansion of virtual memory T cells

In an earlier study, we identified an approximately 3-fold expansion of memory phenotype (MP) $CD8^+$ T cells in mice carrying a spontaneous loss of function mutation in the guanine exchange factor DOCK2 (*Dock2*$^{hsd/hsd}$) (1). This expansion is not specific to this particular allele of *Dock2*, as it is also present in gene targeted *Dock2*-deficient mice (6) (Figure 1A). The increase in the percentage of *Dock2*$^{hsd/hsd}$ MP cells is also mirrored by a similar increase in the total numbers of these cells (Figure 1B). Notably, these cells lack surface expression of NK1.1 and express both CD8α and CD8β (data not shown).

Recent studies have identified cognate antigen-independent memory cells that arise in unmanipulated lymphoreplete mice. (15-17). Such “virtual” memory cells can be distinguished from conventional memory cells by their low expression of CD49d (16). Based on CD49d staining, the majority of expanded memory phenotype Dock2$^{hsd/hsd}$ splenic T cells resemble virtual memory cells (Figure 1C). The ratio of virtual to true memory is also significantly increased in the absence of DOCK2 (Figure 1C).

Dock2$^{hsd/hsd}$ virtual memory cells are functional and their presence correlates with protection from intracellular infection

A key feature of memory cells from antigen-inexperienced mice is the innate-like propensity for the rapid and cognate antigen-independent production of interferon-γ (IFN-γ) following intracellular bacterial infection in response to pro-inflammatory cytokines such as IL-12 and IL-18 or NKG2D ligands (3, 4, 18, 19). Virtual memory T cells are dependent upon IL-15 for their generation, and also require the continued presence of IL-15 in order to maintain the levels of effector molecules necessary for antigen-independent bystander protection (2). Consistent with these studies, a higher proportion of *Dock2*$^{hsd/hsd}$ $CD8^+$ T cells respond rapidly to *in vitro* polyclonal stimuli (PMA + ionomycin, or IL-12 + IL-18) by secreting IFN-γ (Figure 1D and 1E).

As virtual memory cells can robustly traffic to the liver (2), we hypothesized that increased IFN-γ production by *Dock2*-deficient T cells could be protective against infection with *Listeria monocytogenes*, which replicates extensively in the liver. Indeed, expansion of virtual memory cells in the absence of DOCK2 correlated with increased resistance to *L.*

monocytogenes infection, as *Dock2*$^{hsd/hsd}$ mice showed significantly lower bacterial burden 3 days after intravenous infection (Figure 1F). Importantly, there were no differences between wild type and *Dock2*$^{hsd/hsd}$ liver bacterial CFUs 18 hours post-infection, consistent with published studies showing that the protective effect of CD8^{+} derived IFN-γ was manifest only 3 days after infection (3).

Dock2$^{hsd/hsd}$ memory phenotype T cells arise in a hematopoietic-intrinsic manner following thymic egress

Some studies have identified key roles for radio-resistant stromal cells in maintaining peripheral T cell homeostasis (20). With this in mind, we sought to evaluate the contribution of non-hematopoietic cells in the expansion of virtual memory T cells by transferring bone marrow into irradiated RAG-deficient recipients. We found that only recipients of Dock2$^{hsd/hsd}$ bone marrow had a robust expansion of memory cells, while mice that received wild type bone marrow had a much smaller virtual memory compartment (Figure 2A). These experiments could not be performed in the setting of competitive reconstitution as *Dock2*-deficient hematopoietic progenitors exhibit a severe defect in bone marrow reconstitution under competition from wild-type cells due to an impaired response to CXCL12 (21). Indeed, mixed bone marrow chimeras, where wild-type (WT) and *Dock2*$^{hsd/hsd}$ mice bone marrow were co-injected into the same *Rag1*$^{-/-}$ recipient, resulted in ~20:1 hematopoietic reconstitution despite a 1:1 transfer of bone marrow precursors.

In contrast to innate CD8^{+} T cells that are generated prior to thymic egress (22, 23), *Dock2*$^{hsd/hsd}$ virtual memory cells arise in the periphery, as mature CD8^{+}CD4^{-}CD44^{hi} cells are not present in the thymus (Figure 2B). Dock2$^{hsd/hsd}$ deficient naive T cells also show no signs of early effector activation (surface CD69 and CD25 expression) or proliferation (as seen by Ki-67 expression) that accompany conventional true memory cell generation following thymic egress (24) (Figure 2C & 2D).

Dock2$^{hsd/hsd}$ naive T cells directly convert into memory phenotype cells

To explore the mechanism underlying the enhanced generation of *Dock2*$^{hsd/hsd}$ virtual memory cells, we examined the immunological gene signatures in the whole transcriptome profiles of *Dock2*-deficient and WT naive and memory phenotype CD8^{+} T cells using Gene Set Variation Analysis (GSVA) (Figure 3A) (25, 26). Unsurprisingly, genes involved in CD8 memory T cell differentiation were among the top 20 pathways that were differentially enriched between the four conditions. However, we were surprised to find that the same three gene sets associated with memory CD8^{+} T cells as well as one gene set associated with day 15 effectors in the LCMV-Armstrong infection model were also among the top ten pathways that were differentially enriched between wild-type (C57BL/6J) and *Dock2*$^{hsd/hsd}$ naïve CD8^{+} T cells using both GSVA and GSEA analysis (Figure 3B and 3C). In order to assess whether a *bona fide* effector signature was enriched in *Dock2*-deficient naive CD8^{+} T cells, we performed GSEA using custom gene sets that were unique to or shared among the above four gene sets (Figure 3D). We found that only the genes which were common to all four gene sets, or the three memory cells gene sets, were enriched in *Dock2*-deficient naïve CD8^{+} T cells. Furthermore, the gene signature that is specific to day 15 effectors was not enriched in the *Dock2*-deficient naïve CD8 T cells. This suggests that CD8^{+} memory-linked

genes are likely to be upregulated in the day 15 effector CD8 T cell gene set, perhaps because the day 15 effectors in the Kaech et al LCMV infection model include memory cell precursors or have initiated the upregulation of memory-linked genes. Full details of this analysis as well as complete gene lists have been provided in Supplementary Tables 1 and 2. Consistent with the direct conversion of these mutant naïve $CD8^+$ T cells to memory T cells and the bypassing of effector T cell clonal expansion, we observed no enrichment of any other gene sets associated with early T cell activation. Genes associated with activation or exhaustion such as CD137(4-1BB), PD1, TIM3, and LAG3 were also expressed at extremely low levels in from naïve CD8 T cells from wild-type and *Dock2*$^{hsd/hsd}$ mice). The complete RNA-seq dataset is available at NCBI GEO (https://www.ncbi.nlm.nih.gov/geo/query/acc.cgi?acc=GSE135594).

TCR sequencing analysis suggested that the repertoire of the naive $CD8^+$ T cells was comparably diverse in both *Dock2*-deficient and WT mice (Figure 3E). However, the *Dock2*-deficient virtual memory $CD8^+$ cells were more diverse than WT virtual memory cells, suggesting that the conversion to virtual memory cells was a highly polyclonal process in *Dock2*-deficient mice (Figure 3E-G). One measure of antigenic selection in a TCR repertoire is convergence, the number of unique CDR3 sequences encoding the same amino acid sequence (27). In the context of virtual memory T cells, convergence can be interpreted as selection by self-antigens in the periphery. Analysis of the *Dock2*$^{hsd/hsd}$ memory T cell repertoire revealed a significantly lower number of unique CDR3 nucleotide sequences that encode the same amino acid sequence, compared with wild type memory cells (Figure 3H). This decrease in convergence suggests that the self-antigen affinity threshold for entering the virtual memory compartment is lowered in the absence of DOCK2, allowing more “naive” T cells to enter this compartment. Further supporting this conclusion, we found that the TCR Vβ expression profile of *Dock2*$^{hsd/hsd}$ virtual memory cells bore remarkable similarity to naive T cells and is quite distinct from wild type virtual memory cells (Figure 3I).

In order to determine whether Dock2$^{hsd/hsd}$ naive $CD8^+$ T cells have an increased cell intrinsic propensity to convert to virtual memory, we investigated how adoptively co-transferred Dock2$^{hsd/hsd}$ and WT naive T cells respond to homeostatic signals *in vivo*. *Dock2*$^{hsd/hsd}$ T cells transferred into irradiated lymphopenic mice proliferate at a strikingly faster rate than co-transferred WT T cells with concomitant CD44 upregulation (Figure 4A). Importantly, this increased rate of conversion to memory was also observed when naive *Dock2*$^{hsd/hsd}$ T cells were transferred into lymphoreplete mice without any irradiation (Figure 4B).

Surface CD5 levels, a proxy for tonic TCR signalling (28, 29), were significantly higher on naive T cells from Dock2$^{hsd/hsd}$ mice than WT mice (Figure 4C). In addition, Dock2$^{hsd/hsd}$ naive T cells also exhibit lower surface TCR expression (Figure 4C). These findings suggest that an increase in self peptide-MHC triggering may be associated with the expansion of memory phenotype cells. Interestingly, increased CD5 levels are also seen in *Dock2*$^{hsd/hsd}$ CD8 single-positive thymocytes, suggesting that the *Dock2*-deficient cells may receive stronger positively selecting signals. However, this is not accompanied by dramatic changes in the proportions of thymic precursors (Supplementary Figure 1A).

Responsiveness to weak agonists is selectively enhanced in *Dock2*-deficient T cells

As our experiments implicated tonic TCR signaling in driving the conversion to virtual memory, we generated *Dock2*-deficient OT-I transgenic mice (OT-I *Dock2*$^{hsd/hsd}$) to interrogate this phenomenon in the context of a defined TCR repertoire. OT-I *Dock2*$^{hsd/hsd}$ mice were born at Mendelian ratios and exhibited no obvious developmental defects. However, a close examination of T cells in the spleens of these mice revealed a striking accumulation of virtual memory cells, as compared to OT-I mice with normal expression of DOCK2 (Figure 5A, Supplementary Figure 1B). Thus, the *Dock2*-dependent expansion of CD8$^+$ T cells does not require a polyclonal repertoire.

We next measured the responses of naive *Dock2*-deficient OT-I T cells to altered peptide ligands with varying degrees of affinity for the OT-I TCR using the following peptides, listed in increasing order of affinity: SIIGFEKL (G4), SIITFEKL (T4), SIIQFEKL (Q4), and SIINFEKL (N4) (30). We used CD69 upregulation (31) and cytoskeletal remodeling (32, 33) to evaluate TCR-dependent responses. Incubation of splenocytes with strong and intermediate affinity agonists (N4, T4 and Q4) consistently activated OT-I T cells as measured by CD69 upregulation, regardless of DOCK2 expression (Figure 5B-C). However, weak agonist (G4) stimulation resulted in significantly more CD69$^+$ *Dock2*-deficient OT-I T cells when compared to cells from OT-I *Dock2*$^{+/hsd}$ littermates (Figure 5C). *Dock2*-deficient OT-I T cells also exhibited greater reactivity to both weak and intermediate affinity agonists when TCR reactivity was measured in terms of TCR downregulation (Figure 5D).

TCR signaling is associated with actin polymerization and the enrichment of filamentous actin (F-actin) at the immunological synapse. Remodeling of F-actin at the immunological synapse is essential for TCR signaling events (32, 33). The high affinity (N4) peptide induced comparable levels of polymerized actin at the synapse in both *Dock2*-deficient as well as WT OT-I T cells (Figure 5E and 5G). However, in the *Dock2*-deficient OT-I T cells but not wild-type OT-I T cells, the lowest affinity peptide (G4) induced prominent actin polymerization (Figure 5E and 5F). Collectively, these findings suggest that *Dock2*-deficient OT-I T cells have a significantly reduced threshold of TCR activation in response to low affinity peptides.

DISCUSSION

We had previously shown that the loss of DOCK2 results in a prominent expansion of CD8$^+$ blood memory phenotype (MP) cells, and had used this phenotype to identify a loss-of-function *Dock2* genetic variant (*Dock2*$^{hsd/hsd}$) in the commercially available C57BL6/NHsd substrain of C57BL/6 mice (1). In this study, we show that a similar expansion of CD8$^+$ memory T cells is not specific to this *Dock2* mutant allele and is also seen in gene targeted *Dock2* knockout mice (6). In contrast to conventional antigen-experienced memory cells, the majority of *Dock2*$^{hsd/hsd}$ memory T cells exhibit low surface expression of CD49d, originate in the periphery, lack activation makers, and have a highly diverse repertoire without any dominant clones. It can thus be concluded that the MP cells in *Dock2*$^{hsd/hsd}$ mice represent *bona fide* virtual memory cells.

Virtual memory T cell generation and maintenance is dependent on TCR triggering by self-peptide MHC and common γ-chain cytokine derived signals. However, there is little known about negative regulators of the virtual memory compartment (5). In this study, we have provided evidence that DOCK2 sets a threshold for direct entry of naive CD8+ T cells into the virtual memory compartment. We have shown that there is reduced TCR sequence convergence and greater naive-like TCR Vβ usage in the *Dock2*$^{hsd/hsd}$ virtual memory TCR repertoire suggesting that more "naive" TCRs are able to enter this compartment. We found a striking enrichment in gene sets associated with memory differentiation in the genes that are upregulated in *Dock2*$^{hsd/hsd}$ naive CD8+ T cells relative to WT naive T cells. Notably, there was no enrichment of gene sets associated with effector differentiation. We observed an increased propensity of adoptively co-transferred *Dock2*$^{hsd/hsd}$ naive T cells to convert to a memory phenotype in response to homeostatic signals. We also demonstrated that *Dock2*-deficiency increases TCR sensitivity to weak agonists, and a higher level of CD5 observed on *Dock2*$^{hsd/hsd}$ T cells is consistent with enhanced responsiveness to self-peptide MHC *in vivo*.

A prior study by Sanui *et al*. showed that in the absence of DOCK2, MHC-II restricted 2B4 TCR transgenic CD4^{+} T cells exhibit a reduced response to weak agonist peptides (13). However, the interpretation of this experiment may be complicated by the observation that DOCK2 may negatively influence lymphocyte proliferation independent of antigen receptor signaling (34). Besides DOCK2, FYB1 has been shown to negatively regulate the size of the virtual memory compartment (5). However, the relationship between DOCK2 and FYB1 has not yet been studied, and it is formally possible that DOCK2 and FYB1 function in the same or parallel pathways.

It is currently unclear how the loss of DOCK2 sets the threshold for weak agonist TCR stimulation. One possibility is that the decreased interstitial motility (11) observed by *Dock2*$^{-/-}$ T cells results in increased TCR-MHC contact duration. It is possible that increases in antigen presenting cell "residency" time results in increased amounts of TCR triggering and concomitant conversion into memory cells. Another possibility is that the loss of DOCK2 disrupts the cortical network lowering the threshold for activation by weak ligands. Cortical actin forms a dense 100 nm thick layer lining the plasma membrane and can act as a barrier to TCR signaling by restricting the access of intracellular domains of LAT and CD3 to cytosolic signaling mediators such as PLC-γ1 in the absence of CD28 dependent costimulation (35, 36). The TCR and LAT are present in distinct microclusters in resting T cells, and the disruption of actin polymerization results in their activation-promoting aggregation (37). DOCK2 is localized to the cell membrane via its interactions with the phospholipids, PIP3 and phosphatidic acid, and promotes RAC1-mediated actin polymerization (6-8). Therefore, we speculate that disruption of cortical actin in *Dock2*-deficient mice may contribute to the increased TCR responsiveness to weak agonists by promoting the enhanced diffusion of segregated transmembrane proteins such as the TCR and LAT and promote their association with downstream signaling mediators. Further studies on the role of Rac, the GTPase activated by DOCK2, in TCR signaling and virtual memory differentiation following egress into the periphery could also be informative as current studies of this GTPase have been, largely focused on thymic development and homing (38, 39).

In conclusion, we have demonstrated a novel role for DOCK2 in restricting the size of the virtual memory T cell compartment most likely by setting the threshold for responses against weak agonists. DOCK2 deficiency is a rare cause of severe immunodeficiency and early onset infections in humans (40). However, the effect of DOCK2 on virtual memory cells in humans is yet to be determined as the flow cytometric markers for virtual memory in humans are not well established (15, 41). Our findings suggest that any efforts to dampen immune responses using a small molecule inhibitor of DOCK2 should be tempered by an understanding that this protein has pleiotropic effects on peripheral T cell homeostasis (42).

Supplementary Material

Refer to Web version on PubMed Central for supplementary material.

REFERENCES

1. Mahajan VS, Demissie E, Mattoo H, Viswanadham V, Varki A, Morris R, and Pillai S. 2016 Striking Immune Phenotypes in Gene-Targeted Mice Are Driven by a Copy-Number Variant Originating from a Commercially Available C57BL/6 Strain. Cell Rep. 15: 1901–1909. [PubMed: 27210752]
2. White JT, Cross EW, Burchill MA, Danhorn T, McCarter MD, Rosen HR, O'Connor B, and Kedl RM. 2016 Virtual memory T cells develop and mediate bystander protective immunity in an IL-15-dependent manner. Nat. Commun 7: 11291. [PubMed: 27097762]
3. Berg RE, Crossley E, Murray S, and Forman J. 2003 Memory CD8+ T cells provide innate immune protection against Listeria monocytogenes in the absence of cognate antigen. J. Exp. Med 198: 1583–1593. [PubMed: 14623912]
4. Chu T, Tyznik AJ, Roepke S, Berkley AM, Woodward-Davis A, Pattacini L, Bevan MJ, Zehn D, and Prlic M. 2013 Bystander-Activated Memory CD8 T Cells Control Early Pathogen Load in an Innate-like, NKG2D-Dependent Manner. Cell Rep. 3: 701–708. [PubMed: 23523350]
5. Fiege JK, Burbach BJ, and Shimizu Y. 2015 Negative Regulation of Memory Phenotype CD8 T Cell Conversion by Adhesion and Degranulation-Promoting Adapter Protein. J. Immunol. 195: 3119–3128. [PubMed: 26320248]
6. Fukui Y, Hashimoto O, Sanui T, Oono T, Koga H, Abe M, Inayoshi A, Noda M, Oike M, Shirai T, and Sasazuki T. 2001 Haematopoietic cell-specific CDM family protein DOCK2 is essential for lymphocyte migration. Nature 412: 826–831. [PubMed: 11518968]
7. Nishikimi A, Fukuhara H, Su W, Hongu T, Takasuga S, Mihara H, Cao Q, Sanematsu F, Kanai M, Hasegawa H, Tanaka Y, Shibasaki M, Kanaho Y, Sasaki T, Frohman MA, and Fukui Y. 2009 Sequential regulation of DOCK2 dynamics by two phospholipids during neutrophil chemotaxis. Science 324: 384–387. [PubMed: 19325080]
8. Nishikimi A, Kukimoto-Niino M, Yokoyama S, and Fukui Y. 2013 Immune regulatory functions of DOCK family proteins in health and disease. Exp. Cell Res 319: 2343–2349. [PubMed: 23911989]
9. Terasawa M, Uruno T, Mori S, Kukimoto-Niino M, Nishikimi A, Sanematsu F, Tanaka Y, Yokoyama S, and Fukui Y. 2012 Dimerization of DOCK2 is essential for DOCK2-mediated Rac activation and lymphocyte migration. PLoS One 7: e46277. [PubMed: 23050005]
10. Gotoh K, Tanaka Y, Nishikimi A, Inayoshi A, Enjoji M, Takayanagi R, Sasazuki T, and Fukui Y. 2008 Differential requirement for DOCK2 in migration of plasmacytoid dendritic cells versus myeloid dendritic cells. Blood 111: 2973–2976. [PubMed: 18198348]
11. Nombela-Arrieta C, Mempel TR, Soriano SF, Mazo I, Wymann MP, Hirsch E, Martínez-A C, Fukui Y, von Andrian UH, and Stein JV. 2007 A central role for DOCK2 during interstitial lymphocyte motility and sphingosine-1-phosphate-mediated egress. J. Exp. Med. 204: 497–510. [PubMed: 17325199]
12. Gotoh K, Tanaka Y, Nishikimi A, Nakamura R, Yamada H, Maeda N, Ishikawa T, Hoshino K, Uruno T, Cao Q, Higashi S, Kawaguchi Y, Enjoji M, Takayanagi R, Kaisho T, Yoshikai Y, and

Fukui Y. 2010 Selective control of type I IFN induction by the Rac activator DOCK2 during TLR-mediated plasmacytoid dendritic cell activation. J. Exp. Med 207: 721–730. [PubMed: 20231379]

13. Sanui T, Inayoshi A, Noda M, Iwata E, Oike M, Sasazuki T, and Fukui Y. 2003 DOCK2 is essential for antigen-induced translocation of TCR and lipid rafts, but not PKC-theta and LFA-1, in T cells. Immunity 19: 119–129. [PubMed: 12871644]
14. Le Floc'h A, Tanaka Y, Bantilan NS, Voisinne G, Altan-Bonnet G, Fukui Y, and Huse M. 2013 Annular PIP3 accumulation controls actin architecture and modulates cytotoxicity at the immunological synapse. J. Exp. Med 210: 2721–2737. [PubMed: 24190432]
15. White JT, Cross EW, and Kedl RM. 2017 Antigen-inexperienced memory CD8(+) T cells: where they come from and why we need them. Nat. Rev. Immunol .
16. Haluszczak C, Akue AD, Hamilton SE, Johnson LDS, Pujanauski L, Teodorovic L, Jameson SC, and Kedl RM. 2009 The antigen-specific CD8+ T cell repertoire in unimmunized mice includes memory phenotype cells bearing markers of homeostatic expansion. J. Exp. Med 206: 435–448. [PubMed: 19188498]
17. Akue AD, Lee J-Y, and Jameson SC. 2012 Derivation and maintenance of virtual memory CD8 T cells. J. Immunol 188: 2516–2523. [PubMed: 22308307]
18. Berg RE, Cordes CJ, and Forman J. 2002 Contribution of CD8+ T cells to innate immunity: IFN-γ secretion induced by IL-12 and IL-18. Eur. J. Immunol 32: 2807–2816. [PubMed: 12355433]
19. Soudja SM, Ruiz AL, Marie JC, and Lauvau G. 2012 Inflammatory monocytes activate memory CD8(+) T and innate NK lymphocytes independent of cognate antigen during microbial pathogen invasion. Immunity 37: 549–562. [PubMed: 22940097]
20. Roozendaal R, and Mebius RE. 2011 Stromal cell-immune cell interactions. Annu. Rev. Immunol 29: 23–43. [PubMed: 21073333]
21. Kikuchi T, Kubonishi S, Shibakura M, Namba N, Matsui T, Fukui Y, Tanimoto M, and Katayama Y. 2008 Dock2 participates in bone marrow lympho-hematopoiesis. Biochem. Biophys. Res. Commun 367: 90–96. [PubMed: 18157938]
22. Berg LJ 2007 Signalling through TEC kinases regulates conventional versus innate CD8(+) T-cell development. Nat. Rev. Immunol. 7: 479–485. [PubMed: 17479128]
23. Lee YJ, Jameson SC, and Hogquist KA. 2011 Alternative memory in the CD8 T cell lineage. Trends Immunol. 32: 50–56. [PubMed: 21288770]
24. Kaech SM, and Cui W. 2012 Transcriptional control of effector and memory CD8+ T cell differentiation. Nat. Rev. Immunol 12: 749–761. [PubMed: 23080391]
25. Hänzelmann S, Castelo R, and Guinney J. 2013 GSVA: gene set variation analysis for microarray and RNA-seq data. BMC Bioinformatics 14: 7. [PubMed: 23323831]
26. Godec J, Tan Y, Liberzon A, Tamayo P, Bhattacharya S, Butte AJ, Mesirov JP, and Haining WN. 2016 Compendium of Immune Signatures Identifies Conserved and Species-Specific Biology in Response to Inflammation. Immunity 44: 194–206. [PubMed: 26795250]
27. Shugay M, Bagaev DV, Turchaninova MA, Bolotin DA, Britanova OV, Putintseva EV, Pogorelyy MV, Nazarov VI, Zvyagin IV, Kirgizova VI, Kirgizov KI, Skorobogatova EV, and Chudakov DM. 2015 VDJtools: Unifying Post-analysis of T Cell Receptor Repertoires. PLoS Comput. Biol 11: e1004503. [PubMed: 26606115]
28. Azzam HS, Grinberg A, Lui K, Shen H, Shores EW, and Love PE. 1998 CD5 expression is developmentally regulated by T cell receptor (TCR) signals and TCR avidity. J. Exp. Med 188: 2301–2311. [PubMed: 9858516]
29. Azzam HS, DeJarnette JB, Huang K, Emmons R, Park CS, Sommers CL, El-Khoury D, Shores EW, and Love PE. 2001 Fine tuning of TCR signaling by CD5. J. Immunol 166: 5464–5472. [PubMed: 11313384]
30. Salmond RJ, Brownlie RJ, Morrison VL, and Zamoyska R. 2014 The tyrosine phosphatase PTPN22 discriminates weak self peptides from strong agonist TCR signals. Nat. Immunol 15: 875–883. [PubMed: 25108421]
31. Cibrián D, and Sánchez-Madrid F. 2017 CD69: from activation marker to metabolic gatekeeper. Eur. J. Immunol 47: 946–953. [PubMed: 28475283]

32. Kumari S, Depoil D, Martinelli R, Judokusumo E, Carmona G, Gertler FB, Kam LC, Carman CV, Burkhardt JK, Irvine DJ, and Dustin ML. 2015 Actin foci facilitate activation of the phospholipase C-γ in primary T lymphocytes via the WASP pathway. Elife 4.
33. Kumari S, Curado S, Mayya V, and Dustin ML. 2014 T cell antigen receptor activation and actin cytoskeleton remodeling. Biochim. Biophys. Acta 1838: 546–556. [PubMed: 23680625]
34. Wang L, Nishihara H, Kimura T, Kato Y, Tanino M, Nishio M, Obara M, Endo T, Koike T, and Tanaka S. 2010 DOCK2 regulates cell proliferation through Rac and ERK activation in B cell lymphoma. Biochem. Biophys. Res. Commun 395: 111–115. [PubMed: 20350533]
35. Dustin ML, and Davis SJ. 2014 TCR signaling: the barrier within. Nat. Immunol 15: 136–137. [PubMed: 24448571]
36. Tan YX, Manz BN, Freedman TS, Zhang C, Shokat KM, and Weiss A. 2014 Inhibition of the kinase Csk in thymocytes reveals a requirement for actin remodeling in the initiation of full TCR signaling. Nat. Immunol 15: 186–194. [PubMed: 24317039]
37. Lillemeier BF, Mörtelmaier MA, Forstner MB, Huppa JB, Groves JT, and Davis MM. 2010 TCR and Lat are expressed on separate protein islands on T cell membranes and concatenate during activation. Nat. Immunol 11: 90–96. [PubMed: 20010844]
38. Guo F, Cancelas JA, Hildeman D, Williams DA, and Zheng Y. 2008 Rac GTPase isoforms Rac1 and Rac2 play a redundant and crucial role in T-cell development. Blood 112: 1767–1775. [PubMed: 18579797]
39. Dumont C, Corsoni-Tadrzak A, Ruf S, de Boer J, Williams A, Turner M, Kioussis D, and Tybulewicz VLJ. 2009 Rac GTPases play critical roles in early T-cell development. Blood 113: 3990–3998. [PubMed: 19088377]
40. Dobbs K, Domínguez Conde C, Zhang S-Y, Parolini S, Audry M, Chou J, Haapaniemi E, Keles S, Bilic I, Okada S, Massaad MJ, Rounioja S, Alwahadneh AM, Serwas NK, Capuder K, Çiftçi E, Felgentreff K, Ohsumi TK, Pedergnana V, Boisson B, Haskoloğlu Ş, Ensari A, Schuster M, Moretta A, Itan Y, Patrizi O, Rozenberg F, Lebon P, Saarela J, Knip M, Petrovski S, Goldstein DB, Parrott RE, Savas B, Schambach A, Tabellini G, Bock C, Chatila TA, Comeau AM, Geha RS, Abel L, Buckley RH, İkincioğulları A, Al-Herz W, Helminen M, Doğu F, Casanova J-L, Boztuğ K, and Notarangelo LD. 2015 Inherited DOCK2 Deficiency in Patients with Early-Onset Invasive Infections. N. Engl. J. Med 372: 2409–2422. [PubMed: 26083206]
41. Jacomet F, Cayssials E, Basbous S, Levescot A, Piccirilli N, Desmier D, Robin A, Barra A, Giraud C, Guilhot F, Roy L, Herbelin A, and Gombert J-M. 2015 Evidence for eomesodermin-expressing innate-like CD8(+) KIR/NKG2A(+) T cells in human adults and cord blood samples. Eur. J. Immunol 45: 1926–1933. [PubMed: 25903796]
42. Nishikimi A, Uruno T, Duan X, Cao Q, Okamura Y, Saitoh T, Saito N, Sakaoka S, Du Y, Suenaga A, Kukimoto-Niino M, Miyano K, Gotoh K, Okabe T, Sanematsu F, Tanaka Y, Sumimoto H, Honma T, Yokoyama S, Nagano T, Kohda D, Kanai M, and Fukui Y. 2012 Blockade of inflammatory responses by a small-molecule inhibitor of the Rac activator DOCK2. Chem. Biol 19: 488–497. [PubMed: 22520755]
43. Picelli S, Björklund ÅK, Faridani OR, Sagasser S, Winberg G, and Sandberg R. 2013 Smart-seq2 for sensitive full-length transcriptome profiling in single cells. Nat. Methods 10: 1096–1098. [PubMed: 24056875]
44. Subramanian A, Tamayo P, Mootha VK, Mukherjee S, Ebert BL, Gillette MA, Paulovich A, Pomeroy SL, Golub TR, Lander ES, and Mesirov JP. 2005 Gene set enrichment analysis: a knowledge-based approach for interpreting genome-wide expression profiles. Proc. Natl. Acad. Sci. U. S. A 102: 15545–15550. [PubMed: 16199517]
45. Ritchie ME, Phipson B, Wu D, Hu Y, Law CW, Shi W, and Smyth GK. 2015 limma powers differential expression analyses for RNA-sequencing and microarray studies. Nucleic Acids Res. 43: e47. [PubMed: 25605792]
46. Bolotin DA, Poslavsky S, Mitrophanov I, Shugay M, Mamedov IZ, Putintseva EV, and Chudakov DM. 2015 MiXCR: software for comprehensive adaptive immunity profiling. Nat. Methods 12: 380–381. [PubMed: 25924071]
47. Rashidian M, Ingram JR, Dougan M, Dongre A, Whang KA, LeGall C, Cragnolini JJ, Bierie B, Gostissa M, Gorman J, Grotenbreg GM, Bhan A, Weinberg RA, and Ploegh HL. 2017 Predicting

the response to CTLA-4 blockade by longitudinal noninvasive monitoring of CD8 T cells. J. Exp. Med 214: 2243–2255. [PubMed: 28666979]

48. Inaba K, Inaba M, Romani N, Aya H, Deguchi M, Ikehara S, Muramatsu S, and Steinman RM. 1992 Generation of large numbers of dendritic cells from mouse bone marrow cultures supplemented with granulocyte/macrophage colony-stimulating factor. J. Exp. Med. 176: 1693–1702. [PubMed: 1460426]

Key points

1. DOCK2-deficient $CD8^+$ T cells spontaneously convert into virtual memory cells.
2. *Dock2*$^{-/-}$ $CD8^+$ T cells exhibit enhanced responsiveness to weak agonists.

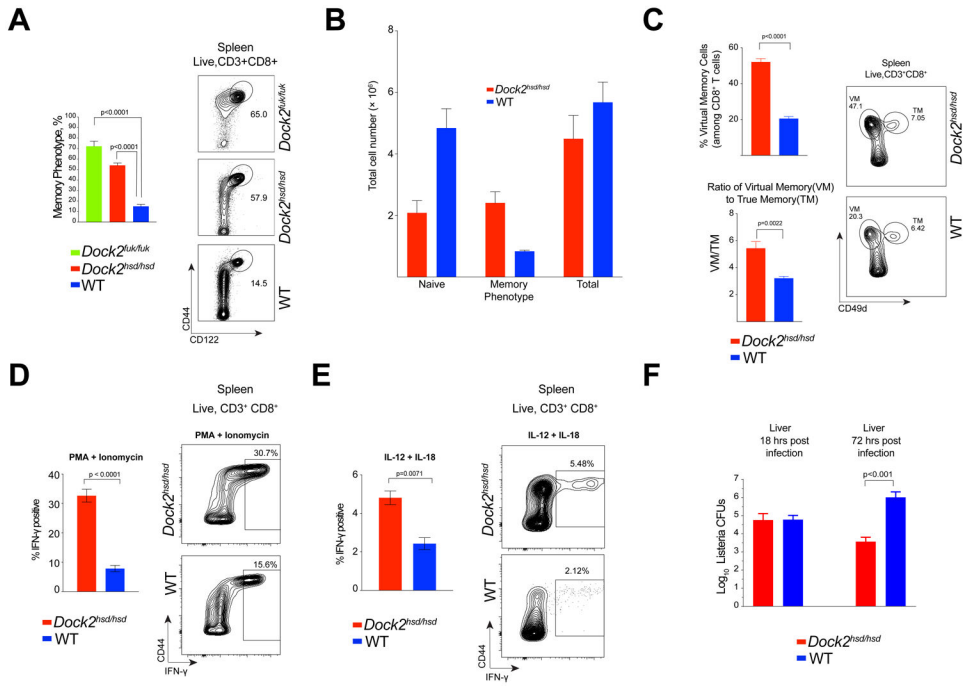

Figure 1: *Dock*$^{hsd/hsd}$ mice have an expanded virtual T cell compartment and are resistant to intracellular bacterial infection with *Listeria monocytogenes*

(A) The proportion of CD8^{+} memory phenotype cells (MP) in the spleens of *Dock2*$^{hsd/hsd}$, *Dock2*$^{Fukui/Fukui}$ and wild-type (WT) mice as measured by flow cytometry.

(B) Number of naive (CD44^{lo}CD122^{-}), memory phenotype (CD44^{hi}CD122^{hi}) and total CD8^{+} T cells in the spleens of WT and *Dock2*-deficient mice.

(C) Percentage of CD8^{+} virtual memory (VM) (CD44^{hi}CD49d^{lo}) T cells among total CD8^{+} T cells as well as the ratio of VM to true memory (TM) (CD44^{hi}CD49d^{hi}) CD8^{+} T cells in the spleens of WT and *Dock2*-deficient mice

(D & E) Intracellular staining for IFN-γ in WT and *Dock2*-deficient CD8^{+} T cells stimulated for 4 hours with PMA and Ionomycin (D) or for 18 hours with IL-12 and IL-18 (E).

(F) Bacterial burden in the livers of *Listeria*-infected WT and *Dock2*-deficient mice at 18 and 72 hours post-infection (data from two experiments with groups of 3 to 4 mice each). In the above experiments, statistical significance was assessed using unpaired two-tailed Student's t test.

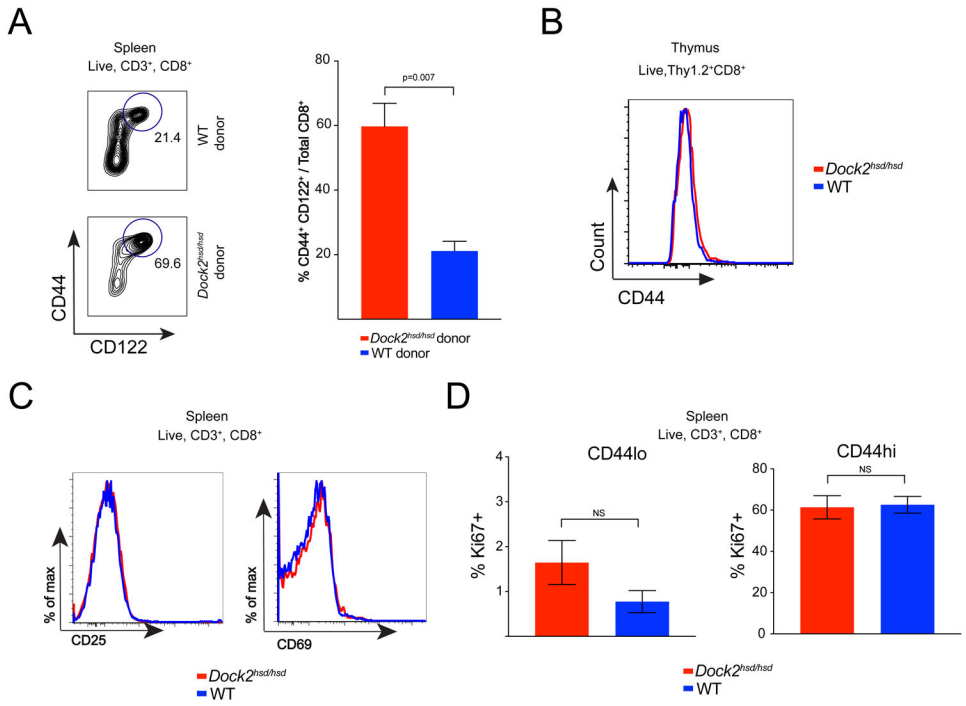

Figure 2: *Dock*$^{hsd/hsd}$ virtual memory T cells arise in a cell-intrinsic manner following thymic egress

(A) Bone marrow cells from either *Dock2*$^{hsd/hsd}$ or WT mice were injected into irradiated *Rag1*$^{-/-}$ mice. The spontaneous generation of memory CD8^{+} T cells (CD44^{hi} CD122^{hi}) was examined in the recipient mice at 12 weeks after cell transfer.

(B) CD44 levels on the Thy1.2^{+} CD8^{+} CD4^{-} single positive thymocytes from WT and *Dock2*-deficient mice.

(C) Levels of activation markers (CD25 and CD69) on splenic CD8^{+} T cells from WT and *Dock2*-deficient mice

(D) Percentage of Ki-67+ cells in the CD44^{lo} and CD44^{hi} CD8^{+} T cell compartments in WT and *Dock2*-deficient mice.

All experiments were performed twice in groups of 3 to 4 mice. Statistical significance was assessed using unpaired two-tailed Student's t-test.

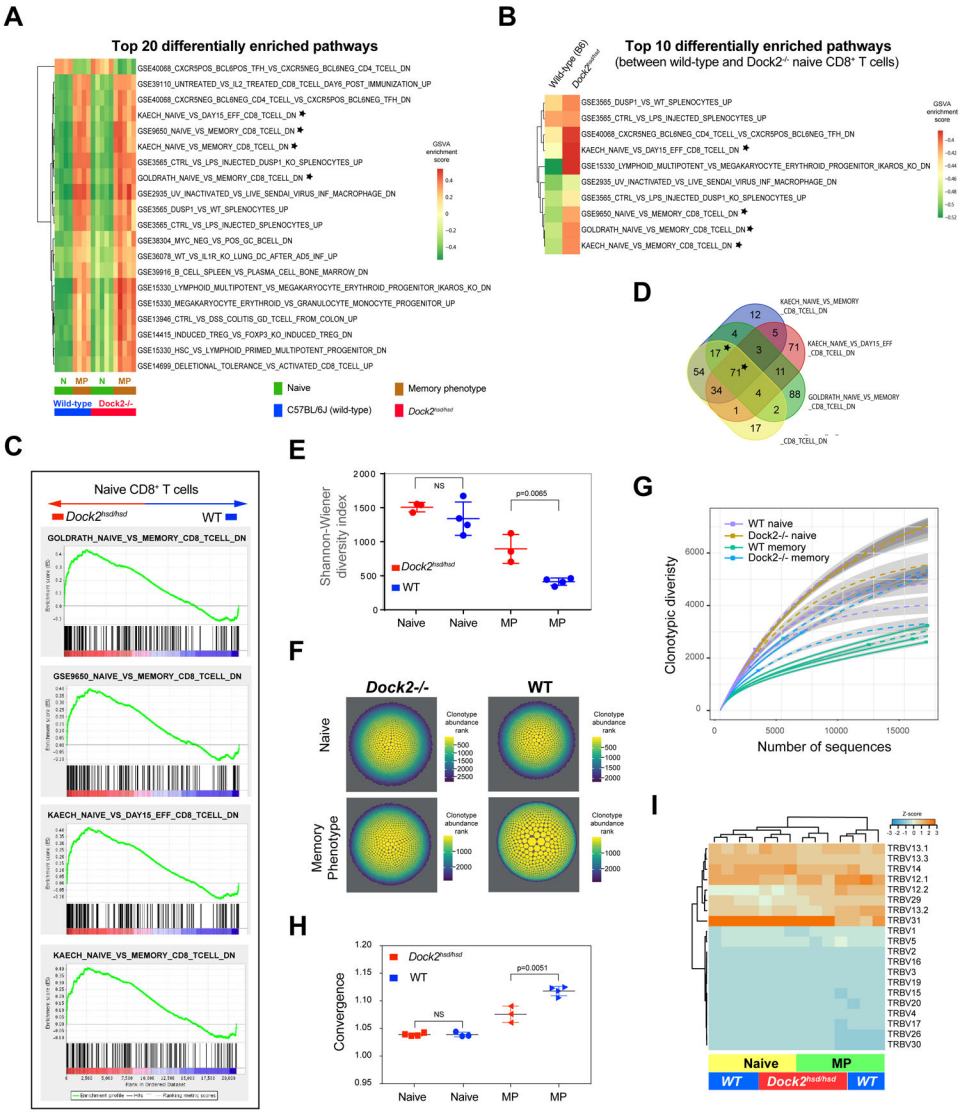

Figure 3: Naïve *Dock2*$^{hsd/hsd}$ T cells exhibit memory-like characteristics

(A) Top twenty differentially enriched immunological gene signatures among naïve and memory phenotype CD8^{+} T cells from wild-type and *Dock2*$^{hsd/hsd}$ mice.

(B) Top ten differentially enriched immunological gene signatures between wild-type and *Dock2*$^{hsd/hsd}$ naïve CD8^{+} T cells. Gene sets linked to memory T cell differentiation are marked with a star in A and B. In both A and B, the heatmaps are colored by the GSVA enrichment score.

(C) Gene set enrichment analysis of genes upregulated in CD8^{+} naive (CD44^{lo}CD122^{--}) *Dock2*$^{hsd/hsd}$ T cells compared to WT naive CD8^{+} T cells. Significantly enriched pathways linked to memory T cell differentiation are shown.

(D) Overlap among the enriched gene sets linked to memory CD8^{+} T cell differentiation shown in A, B and C. Only the starred overlaps are significantly enriched in naive CD8^{+} (CD44^{lo}CD122^{--}) *Dock2*$^{hsd/hsd}$ T cells compared to wild-type by GSEA analysis.

(E,F and G) The repertoire diversity of naïve and memory phenotype (MP) $CD8^+$ T cells from *Dock2*-deficient and wild-type mice assessed using the Shannon-Wiener diversity index (E) and visualized by scaling the area and color of the clonotypes by their abundance (F) or using a rarefaction plot (G).

(H) Repertoire convergence (F) (i.e. number of unique CDR3 nucleotide sequences that encode the same amino acid sequence) in naive ($CD44^{lo}CD122^-$) and MP ($CD44^{hi}CD122^+$) T cells from WT and $Dock2^{hsd/hsd}$ mice. Statistical significance was assessed using unpaired two-tailed Student's t test.

(I) A hierarchically clustered heatmap of the frequency of TCR Vβ gene segment usage in naive ($CD44^{lo}CD122^{--}$) and MP ($CD44^{hi}CD122^+$) $CD8^+$ T cells from $Dock^{hsd/hsd}$ and WT mice.

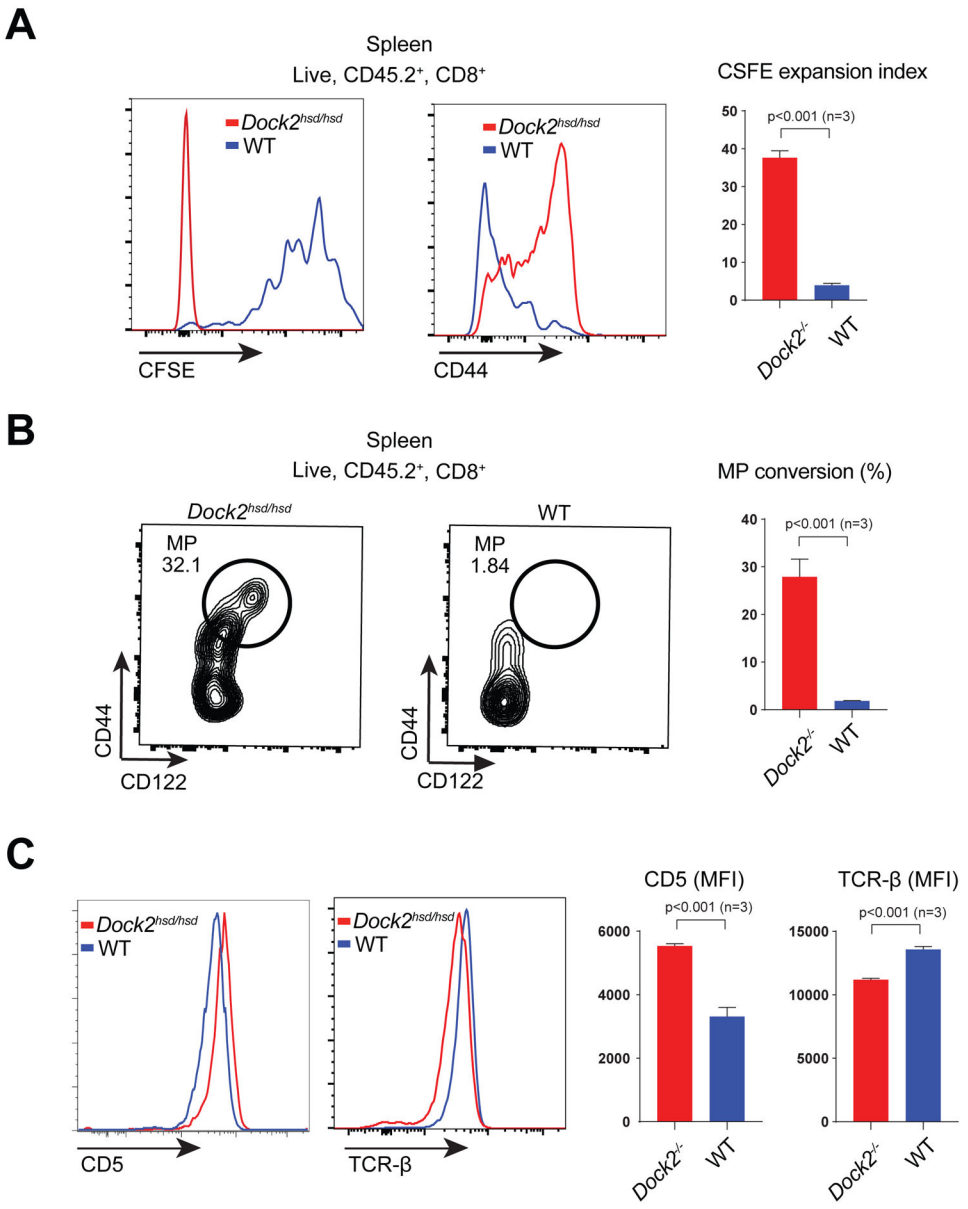

Figure 4: Naïve *Dock2*$^{hsd/hsd}$ T cells undergo spontaneous conversion into virtual memory T cells

(A) Naive T cells from CD45.2$^+$ Thy1.2$^+$ *Dock2*$^{hsd/hsd}$ and CD45.2$^+$ Thy1.1$^+$ WT mice were co--transferred into irradiated CD45.1$^+$ Thy1.2$^+$ lymphopenic mice and assessed for CFSE dilution and CD44 upregulation after 1 week.

(B) Naive T cells from CD45.2$^+$ Thy1.2$^+$ *Dock2*$^{hsd/hsd}$ and CD45.2$^+$ Thy1.1$^+$ WT mice were co-transferred into unmanipulated lymphoreplete CD45.1$^+$ Thy1.2$^+$ mice and assessed for upregulation of memory markers after 3 weeks.

(C) Surface levels of CD5 and TCR on naive CD8$^+$ T cells from *Dock2*$^{hsd/hsd}$ and WT mice as assessed by flow cytometry.

Statistical significance was assessed using unpaired two-tailed Student's t-test.

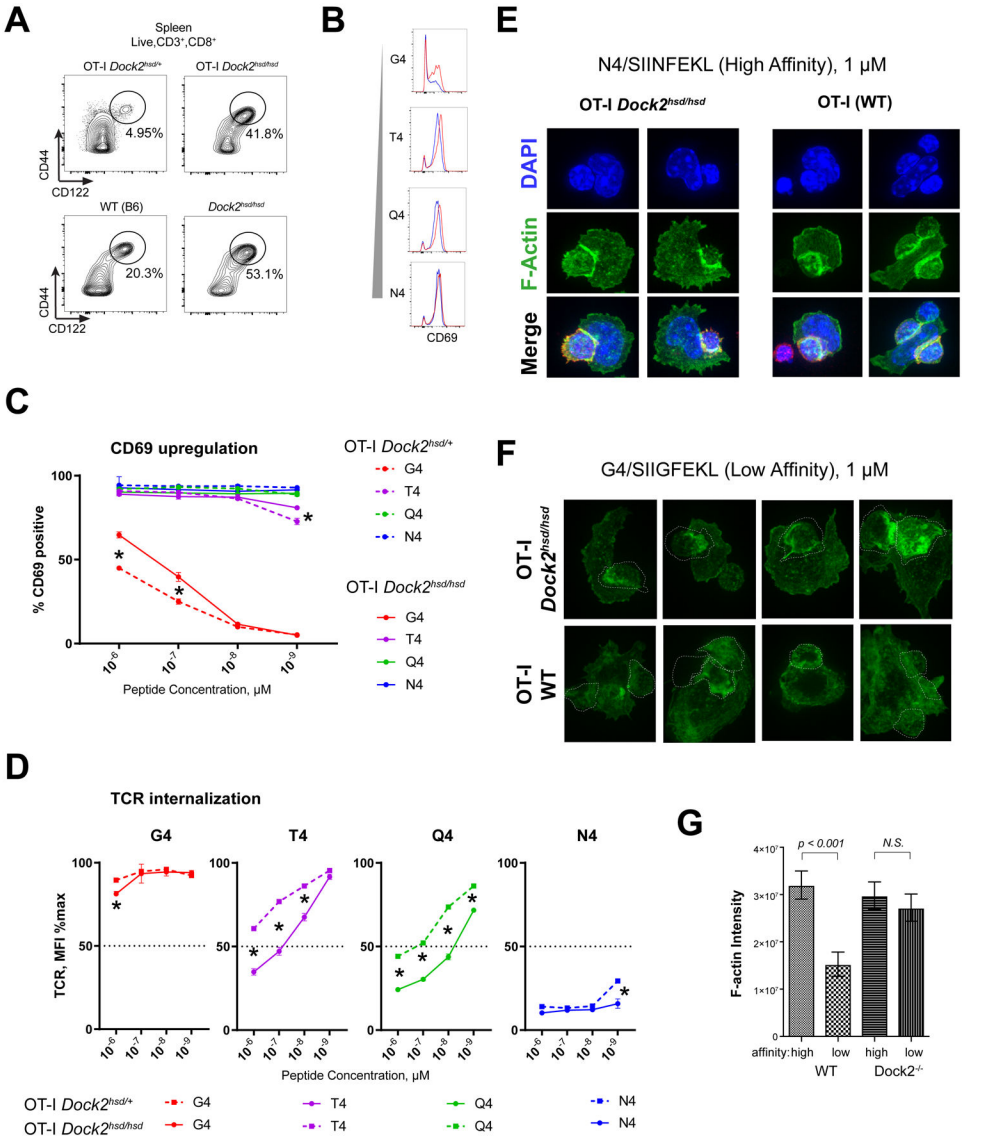

Figure 5: OT-I *Dock2*$^{hsd/hsd}$ mice have an expansion of memory phenotype (MP) T cells and show increased *ex vivo* responses to TCR stimulation

(A) The proportion of CD8^{+} CD44^{hi} CD122^{+} memory phenotype (MP) cells in the spleens of OT-I TCR-transgenic mice in the WT and *Dock2*$^{hsd/hsd}$ background.

(B-D) T cell activation in response to four hours of ex vivo stimulation with peptides of varying signal TCR affinity. Representative histograms in response to stimulation with 1μM peptide (B). Percentage of CD69^{+} cells observed (C) or degree of TCR downregulation (D) in response to a range of peptide concentrations. Statistically significant differences ($p < 0.001$) assessed using an unpaired t-test are marked with asterisks.

(E and F) Confocal microscopy of filamentous actin (green) at the immunological synapse in OT-I WT or OT-I *Dock2*$^{hsd/hsd}$ T cells co-cultured with syngeneic wild-type splenocytes in presence of (C) the high affinity SIINFEKL (N4) peptide or (D) the low affinity SIIGFEKL (G4) peptide. OT-I T cells were pre-stained with a fluorescently labeled anti-CD8 nanobody (red).

(G) Quantification of F-actin intensity in OT-I WT and *Dock2*$^{hsd/hsd}$ CD8^{+} T cells upon stimulation with high (N4) or low (G4) affinity peptides shown as integrated fluorescence intensity. The Mann–Whitney unpaired t-test was used to assess statistical significance. The bars charts depict mean ± SEM.